# Evaluation of weather data at different spatial and temporal scales on fire behaviour prediction using PHOENIX RapidFire 4.0 - Kilmore Case Study

## Technical Report

A report prepared by:

Derek Chong (University of Melbourne/Bushfire CRC)
Thomas Duff (Bushfire CRC)
Kevin Tolhurst (University of Melbourne)

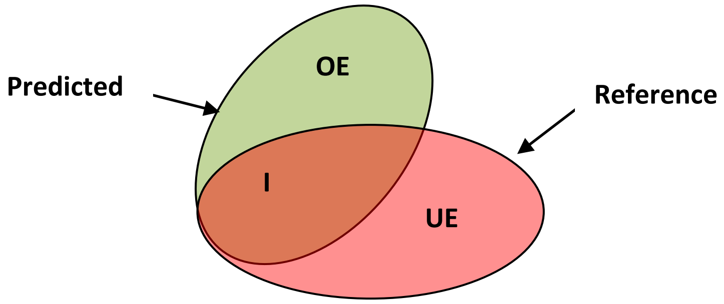

| | |
|---|---|
| Theme: | Understanding Risk |
| Project: | Fire Impact and Risk Evaluation Decision Support Tool |
| Component: | Enhancement of Fire Behaviour Models |
| Milestone: | 3.2.2 and Commonwealth 1.2.5 |
| Date: | 13 September 2012 |

**Cover image:** Diagram showing the components of the Area Difference Index used to compare a predicted fire area with the observed fire area. The ADI is novel and was developed for this project.

This report was produced with financial support from the Bushfire CRC. This is not a published report and has had internal review, but not independent external peer review. Any opinions expressed in this report are those of the authors and not the University of Melbourne or the Bushfire CRC. Any use of original concepts, ideas or results in this report should be done in consultation with the authors.

# Summary

High resolution models might be expected to produce more accurate predictions, but in the case of weather forecasting data used to predict the spread of the 2009 Kilmore fire, this was not found to be true.

Current weather forecasts are available on a 3600 m grid at hourly intervals. In time, computing power will enable finer spatial and temporal forecast weather to be produced operationally. This study was undertaken to understand what benefit finer scaled data might be to fire spread prediction.

PHOENIX RapidFire was used to model the 2009 Kilmore fire with different spatial and temporal weather inputs. Because the fire of this size interacts with the local weather, it was found that courser level weather inputs performed better than very fine resolution data. Overall, weather forecasts at 30 minutes intervals and 1200 m spacing provided the best inputs for matching the progression of the fire. Once the fire had reached about 100,000 ha, 60 minute, 3600 m data gave the best predictions.

Modelling weather at 400 m resolutions and at 5 minute intervals provides good insights into the dynamics of the weather which assists a weather forecaster, but that additional detail is not of the same benefit to fire spread predictions because large fires "smooth" the weather, terrain and fuel in the landscape.

More case-studies need to be undertaken, including smaller fires burning under milder conditions to better understand the relationship between weather data scale and fire spread prediction.

# Contents

Summary ........................................ 0
Contents ........................................ 1
Introduction ........................................ 2
Gridded Weather Data ........................................ 3
Fire Progression Comparison - Area Difference Index ........................................ 4
2009 Kilmore Fire Reconstruction Data ........................................ 6
Forecast Weather Evaluation ........................................ 7
Conclusions ........................................ 15
References ........................................ 16

# Introduction

Currently the Bureau of Meteorology uses the ACCESS numerical prediction model to produce forecast weather grids at hourly time steps and in spatial grids approximately 2-6 km square dependent on the size of the State. Processing time constraints limit the modeled spatial and temporal resolution for operational use. However, for the purposes of this project, the forecast grids were produced at finer spatial and temporal intervals for evaluation.

The purpose of this report is to compare the effect of different spatial and temporal gridded weather resolutions on the spread of the Kilmore fire using the PHOENIX fire characterization model.

## Gridded Weather Data

The Bureau of Meteorology supplied ACCESS model runs for the study area at 3 spatial resolutions (400, 1200 and 3600 m) at 5 minute time steps for evaluation. Raw ACCESS runs exhibited a significant wind speed bias underestimating 10 m wind speed by up to a factor of 1.7 at all resolutions when compared with the Kilmore Gap observations at the AWS location.

The gridded data wind speeds were subsequently bias corrected by Geoscience Australia to better match the observed values (Fig.1).

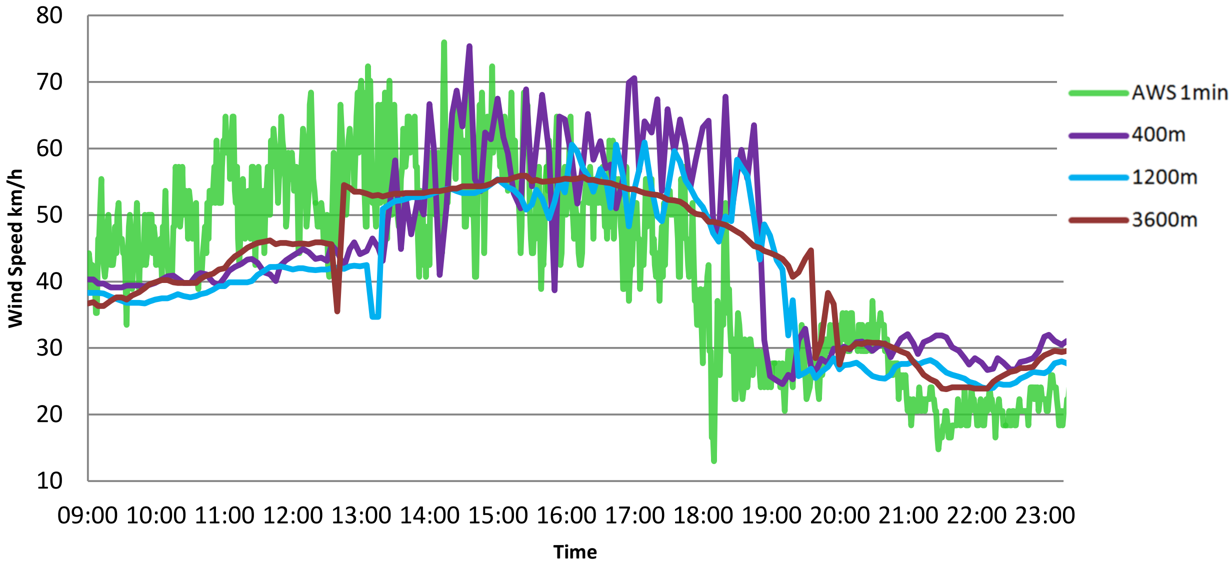

**Figure 1.** Bias corrected wind speeds for 5 minute, 400, 1200 and 3600 m grids compared to 1 minute observations at Kilmore Gap automatic weather station AWS.

The other significant issue with the ACCESS model runs was in the timing of the change which is modeled at between 1 hour (400 m) and 1 hour 40 minutes later than observed (Fig.2).

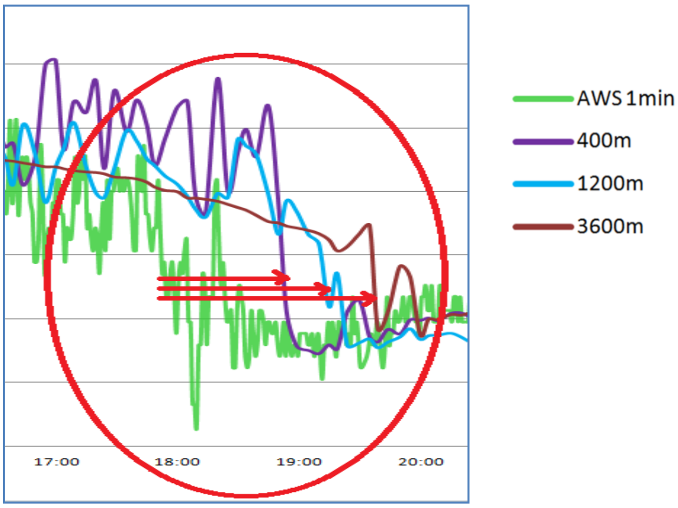

**Figure 2.** Red arrows showing difference in time of change compared to 1 minute observations in green

Initially, offsetting the grids temporally was considered, however this would have introduced significant biases in the other weather values, namely temperature and RH. To avoid the significant errors that would result from the time of change bias PHOENIX model runs were restricted to pre-change conditions, ending at 1800h.

## Fire Progression Comparison - Area Difference Index

The comparison of fire perimeters is a unique problem in morphometric analysis, as while perimeters being compared typically share a common origin, there are few other distinct features that can be used as ‘landmarks’ for objective analysis. There has been limited research into the most appropriate ways to compare fire perimeters, and consequently most comparisons are limited to subjective descriptions or consideration of only the area overlapped by both shapes. For scientifically defensible outcomes, comparisons must be objective, consistent and repeatable. To enable automated fire evaluation, evaluations must also be robust and able to consider a wide variety of perimeter shapes, including fires consisting of multiple parts (such as those generated through spotting). For effective model calibration, the impact of any change to model function should be assessed as the weighted change in performance when considering all training fires. Such systematic evaluation processes do are not compatible with subjective evaluations of fit.

As a consequence, a modified index based on the Shape Deviation Index (SDI, Cui and Perrera, 2010) was selected for used. The SDI is an index of the difference between a test perimeter and reference perimeter, found by evaluating the sum of the area over predicted (the area where the test fire had burned, but the reference had not) and the area under predicted (where the reference fire had burned but the test fire had not), divided by the area of the test fire. The SDI at time ‘t’ can be represented by:

$$SDI\ (t) = \frac{OE(t) + UE(t)}{F(t)}$$

Where OE =Overestimate, UE = Underestimate and F = the area of the observed fire (Fig 3). SDI is an unbounded ratio, with a perfect fit being 0 and poorer fits resulting in larger numbers.

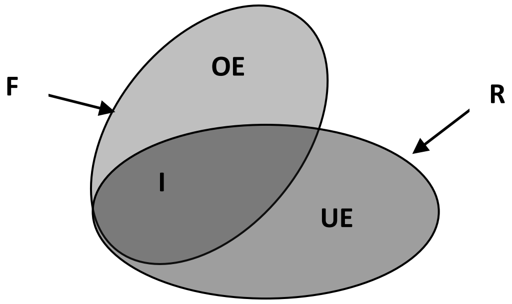

Figure 3. Fire metrics evaluated using SDI and ADI. F = Test fire, R = Reference fire, OE = Overestimate, UE = Underestimate, I = Intersection.

However, the inclusion of F, the observed fire area, as the denominator in the SDI calculation reduces the value of the index. With F as the denominator, the SDI becomes asymmetrical; comparing fire perimeters A and B will yield a different result to comparing fires B and A. In addition, including the total area of the test fire as the denominator in essence rewards underprediction, as the SDI will approach 1 as the total area of F increases relative to the area correctly predicted.

As a result, we are using a modified form of the SDI, the Area Difference Index (ADI). The ADI is similar to the SDI, however rather than using the test fire area as the denominator, the intersection area (the area common to both fires) is used. This scales the ADI proportional to the area of interest (the correctly predicted area) and results in a symmetrical index that no longer rewards underprediction. As with the SDI, the ADI is an unbounded ratio, with 0 as a perfect fit and poorer fits resulting in larger numbers. An ADI of 1 indicates that the sum of the areas poorly predicted (over and under) is equal to the correctly predicted area (intersection).

$$ADI\ (t) = \frac{OE(t) + UE(t)}{I(t)}$$

Where OE =Overestimate, UE = Underestimate and I = the area of the intersection.

## 2009 Kilmore Fire Reconstruction Data

The Kilmore fire reconstruction data was obtained from the Victorian Department of Sustainability and Environment (DSE), specifically the digitized fire progression lines. In order to compare PHOENIX modeled progression with the DSE linework, the fire progression lines were first converted to time stamped polygons.

Progression lines were first generalized using the ArcGIS Simplify Polygon tool to ensure perimeter point resolution did not exceed ArcGIS 0.0001 meter tolerance. Minimum allowable offset was set at 1 meter. Failure to do this can result in anomalous results when using GIS tools. Initially no generalization was performed on the perimeter 'lines' which resulted in polygons being dropped when merging with no error message provided.

On closer investigation of the progression lines it was discovered that several perimeters were missing significant segments with only the active fire fronts mapped. To convert these to polygons it was assumed that the previous complete polygon captured the missing segments, these were manually digitized in ArcGIS.

In addition, several isolated ‘sub’ time step progressions had also been mapped. Numerical comparison between modeled and observed requires a coherent fire footprint at a point in time to be supplied. Only progression lines meeting this requirement were used (Table 1).

**Table 1. Times of the 18 fire progression observations used**

| Observation Time |
|---|
| 7/02/2009 11:50 AM |
| 7/02/2009 12:00 PM |
| 7/02/2009 12:15 PM |
| 7/02/2009 12:20 PM |
| 7/02/2009 12:48 PM |
| 7/02/2009 12:55 PM |
| 7/02/2009 1:46 PM |
| 7/02/2009 2:40 PM |
| 7/02/2009 2:45 PM |
| 7/02/2009 3:15 PM |
| 7/02/2009 3:30 PM |
| 7/02/2009 4:00 PM |
| 7/02/2009 4:25 PM |
| 7/02/2009 5:00 PM |
| 7/02/2009 5:10 PM |
| 7/02/2009 5:30 PM |
| 7/02/2009 5:50 PM |
| 7/02/2009 6:00 PM |

The ArcGIS 10 ‘Feature to Polygon’ tool was used to convert linear features to polygons, but this process drops all attributes in its conversion. This meant that each observation time step had to be exported as a separate shapefile before conversion to polygon. After conversion, a Date_Time column was added and the observation time added. The individual files where then re combined using the merge function.

## Forecast Weather Evaluation

PHOENIX model sensitivity to ACCESS runs of Black Saturday weather at 400, 1200 and 3600 m were evaluated at 5, 15, 30 and 60 minute time steps. The 15, 30 and 60 minute data supplied by Geoscience Australia was extracted from the 5 minute data at the specified intervals, no averaging or interpolation was performed. The resulting fire progressions were compared against the 18 supplied reconstruction perimeters.

Weather data were extracted at 10 m above surface for wind speed and direction, and screen height (1.2 m) for temperature and relative humidity. Drought factor was assumed to be 10 and curing was set at 100% which is consistent with the findings of the reconstruction report for spread until 18:00.

The convention used to identify weather dataset was xxxx_Txx where the first component representing the gridded weather resolution in meters and the second prefixed with the letter 'T' indicating the time step. This convention is used in Table 2.

**Table 2. ADI over time by weather resolution and time step (11:45 am ignition time), lower ADIs indicate a better fit. The best fit for each time interval is shown in yellow.**

| DateTime | 400_T5 | 400_T15 | 400_T30 | 400_T60 | 1200_T5 | 1200_T15 | 1200_T30 | 1200_T60 | 3600_T5 | 3600_T15 | 3600_T30 | 3600_T60 |
|---|---|---|---|---|---|---|---|---|---|---|---|---|
| **11:50** | 47.85 | 49.02 | 48.14 | 44.11 | 38.57 | 37.51 | 38.41 | 38.21 | 33.71 | 34.06 | 34.42 | 35.73 |
| **12:00** | 6.55 | 7.01 | 6.89 | 6.25 | 4.48 | 4.45 | 4.43 | 4.33 | 2.35 | 2.34 | 2.38 | 2.48 |
| **12:15** | 2.56 | 2.49 | 2.46 | 2.36 | 2.07 | 1.95 | 2.24 | 1.82 | 4.04 | 4.16 | 4.12 | 4.07 |
| **12:20** | 4.05 | 4.58 | 3.53 | 3.72 | 2.63 | 2.31 | 2.99 | 1.98 | 5.33 | 5.33 | 5.42 | 5.19 |
| **12:48** | 1.96 | 4.30 | 1.33 | 2.85 | 1.42 | 1.36 | 1.79 | 1.21 | 4.35 | 3.02 | 4.26 | 3.84 |
| **12:55** | 1.72 | 4.26 | 1.45 | 2.74 | 1.43 | 1.61 | 1.89 | 1.31 | 4.34 | 3.05 | 4.09 | 3.72 |
| **13:46** | 1.53 | 1.56 | 1.66 | 2.06 | 1.86 | 2.32 | 2.58 | 1.71 | 5.03 | 3.62 | 3.47 | 3.39 |
| **14:40** | 1.21 | 1.40 | 1.31 | 1.33 | 1.62 | 1.53 | 1.68 | 1.14 | 2.92 | 1.69 | 2.06 | 1.90 |
| **14:45** | 1.84 | 2.11 | 1.82 | 1.33 | 1.99 | 1.09 | 1.78 | 2.15 | 1.23 | 1.14 | 0.86 | 0.90 |
| **15:15** | 2.53 | 3.17 | 2.84 | 1.45 | 2.94 | 1.35 | 2.26 | 2.19 | 1.39 | 1.27 | 0.92 | 0.90 |
| **15:30** | 3.21 | 4.09 | 3.41 | 1.88 | 3.52 | 1.21 | 2.47 | 2.75 | 1.12 | 1.02 | 0.76 | 0.78 |
| **16:00** | 3.22 | 3.32 | 3.11 | 1.92 | 2.92 | 0.68 | 2.28 | 2.95 | 1.16 | 0.73 | 0.84 | 0.68 |
| **16:25** | 3.81 | 3.67 | 3.58 | 2.02 | 3.44 | 0.68 | 2.09 | 3.02 | 0.99 | 0.74 | 0.75 | 0.64 |
| **17:00** | 2.51 | 3.86 | 3.39 | 1.20 | 2.36 | 0.97 | 1.76 | 2.24 | 0.72 | 0.70 | 0.67 | 0.60 |
| **17:10** | 2.10 | 3.56 | 3.03 | 1.01 | 2.25 | 0.87 | 1.49 | 2.03 | 0.71 | 0.65 | 0.63 | 0.55 |
| **17:30** | 1.77 | 2.80 | 2.04 | 0.96 | 1.94 | 0.91 | 1.44 | 1.72 | 0.60 | 0.66 | 0.64 | 0.61 |
| **17:50** | 1.65 | 2.20 | 1.76 | 1.06 | 1.85 | 1.06 | 1.54 | 1.47 | 0.62 | 0.72 | 0.75 | 0.69 |
| **18:00** | 2.02 | 2.55 | 2.02 | 1.29 | 2.27 | 1.36 | 1.81 | 1.74 | 0.68 | 0.86 | 0.88 | 0.77 |

Table 2 shows the values of the Area Difference Index (ADI) for the various dataset used and for each timestep in the fire development. Initial modeled perimeters at 11:50 differ quite considerably from the reconstructed perimeter across all resolutions, two contributors to this are:

- use of the 11:45 ignition time reported in the reconstruction data. PHOENIX models fires assuming the time supplied is the actual ignition time and includes including a build up phase where as recorded fire ignition times are generally the time the fire was reported which is often several minutes after the ignition.
- Incorrect fuel classification shows an area downwind of the ignition mapped as a forest fuel type where a faster spreading grass fuel is more appropriate.

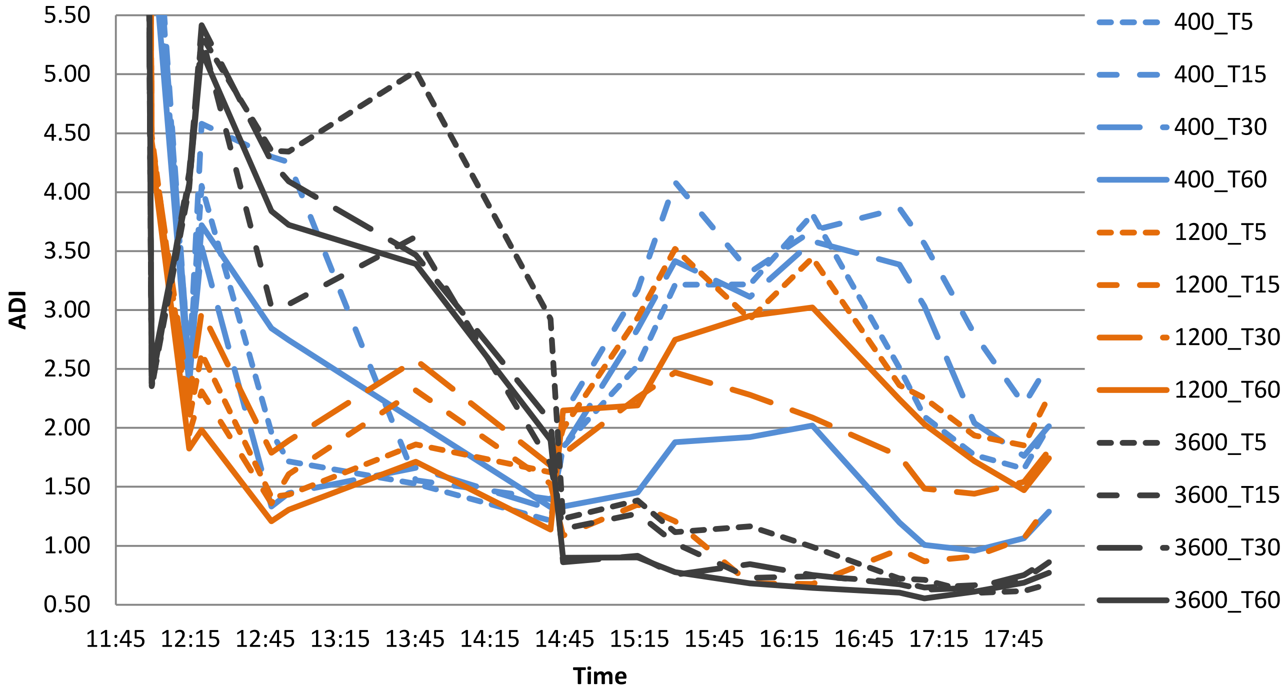

Figure 4. ADI graphed over time comparing the different fire extents predicted when using different spatial and temporally resolved forecast weather data as input (11:45 am ignition time).

Fires were re run with a 11:40 ignition time to compensate for the reporting time and incorrect fuel type. The resulting ADI data shows a significant improvement in the 11:50 match and comparable results for the remaining observations.

**Table 3 ADI over time by weather resolution and time step (11:40 am ignition time). The best fit in each timestep is coloured yellow.**

| DateTime | 400_T5 | 400_T15 | 400_T30 | 400_T60 | 1200_T5 | 1200_T15 | 1200_T30 | 1200_T60 | 3600_T5 | 3600_T15 | 3600_T30 | 3600_T60 |
|---|---|---|---|---|---|---|---|---|---|---|---|---|
| **11:50** | 6.30 | 6.21 | 6.22 | 5.26 | 3.52 | 3.49 | 3.56 | 3.42 | 2.39 | 2.53 | 2.63 | 3.05 |
| **12:00** | 2.34 | 2.28 | 2.36 | 1.93 | 1.29 | 1.25 | 1.24 | 1.25 | 1.32 | 1.25 | 1.27 | 1.30 |
| **12:15** | 1.99 | 2.07 | 2.06 | 2.03 | 1.55 | 1.52 | 1.53 | 1.57 | 3.23 | 3.01 | 2.96 | 3.34 |
| **12:20** | 3.65 | 3.81 | 3.49 | 3.44 | 1.66 | 1.74 | 1.67 | 1.71 | 2.99 | 2.76 | 2.68 | 3.13 |
| **12:48** | 3.37 | 3.87 | 2.49 | 2.44 | 1.20 | 1.26 | 1.19 | 1.35 | 2.41 | 3.01 | 2.60 | 2.88 |
| **12:55** | 3.08 | 3.56 | 2.16 | 2.54 | 1.44 | 1.36 | 1.42 | 1.59 | 2.81 | 3.24 | 2.78 | 3.19 |
| **13:46** | 1.54 | 1.81 | 1.59 | 1.78 | 1.85 | 1.82 | 1.49 | 1.99 | 3.05 | 3.41 | 3.29 | 3.14 |
| **14:40** | 1.66 | 1.06 | 1.39 | 1.79 | 1.44 | 1.69 | 0.71 | 1.25 | 1.51 | 1.32 | 2.14 | 1.42 |
| **14:45** | 2.10 | 1.48 | 1.86 | 1.84 | 1.15 | 1.98 | 0.55 | 1.59 | 0.97 | 1.07 | 1.53 | 0.74 |
| **15:15** | 2.98 | 1.84 | 2.32 | 2.44 | 1.52 | 2.95 | 0.77 | 2.33 | 1.34 | 1.15 | 1.60 | 0.86 |
| **15:30** | 3.52 | 2.23 | 2.80 | 3.06 | 1.55 | 3.60 | 0.67 | 2.70 | 1.19 | 0.95 | 1.57 | 0.73 |
| **16:00** | 3.55 | 2.67 | 2.74 | 2.86 | 0.78 | 3.18 | 0.62 | 3.09 | 0.76 | 0.58 | 1.14 | 0.77 |
| **16:25** | 3.50 | 3.29 | 2.90 | 3.31 | 0.92 | 3.21 | 0.67 | 3.50 | 0.95 | 0.64 | 0.83 | 0.60 |
| **17:00** | 2.13 | 2.79 | 2.00 | 2.71 | 1.02 | 1.90 | 0.93 | 2.86 | 0.83 | 0.69 | 0.73 | 0.52 |
| **17:10** | 2.05 | 2.61 | 1.68 | 2.70 | 1.04 | 1.66 | 0.82 | 2.78 | 0.78 | 0.65 | 0.66 | 0.50 |
| **17:30** | 1.87 | 2.19 | 1.36 | 1.97 | 1.07 | 1.43 | 0.72 | 1.97 | 0.72 | 0.66 | 0.66 | 0.57 |
| **17:50** | 1.78 | 1.98 | 1.15 | 1.76 | 1.13 | 1.39 | 0.82 | 1.79 | 0.75 | 0.73 | 0.71 | 0.67 |
| **18:00** | 1.85 | 2.37 | 1.39 | 2.05 | 1.36 | 1.59 | 1.00 | 2.12 | 0.88 | 0.90 | 0.86 | 0.85 |

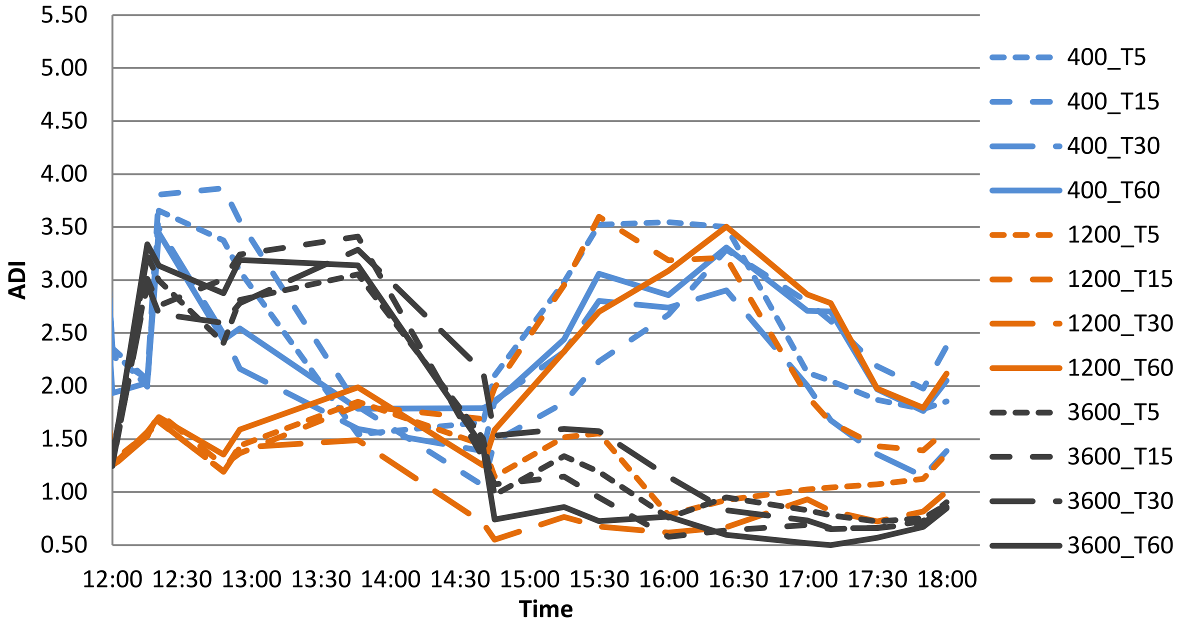

**Figure 5.** ADI graphed over time comparing the effect of different spatial and temporal weather data on the modelled fire extent (11:40 am ignition time).

Initially the higher resolutions generally perform better than the 3600 m data. However, after the 14:45 observation the lower 3600 m data results in a sudden improvement whilst the higher resolutions generally worsen. Using an 11:40 ignition this pattern is essentially repeated except for the 1200_T5 and 1200_T30 runs which perform quite consistently for the duration of the run. 1200 m results are inconsistent however with the T15 and T60 runs mimicking the 400 m runs which worsen after the 14:45 observation.

Looking at the averaged ADI values weighted by modeled area for each resolution show the 3600 m data generally outperforms the higher resolutions. In addition, the final 18:00 ADI values for the 3600 m runs are tightly clustered indicating strong agreement in comparison to the relatively high ADI variability in the 400 m and 1200 m runs.

Table 4. Area-weighted-average ADI values for 11:45 and 11:40 ignitions modeled to 18:00

| Input | ADI_1145 | ADI_1140 |
|---|---|---|
| 3600_T5 | 0.818 | 0.860 |
| 3600_T15 | 0.781 | 0.779 |
| 3600_T30 | 0.797 | 0.838 |
| 3600_T60 | 0.714 | 0.694 |
| 1200_T5 | 2.231 | 1.137 |
| 1200_T15 | 1.038 | 1.736 |
| 1200_T30 | 1.695 | 0.829 |
| 1200_T60 | 1.886 | 2.251 |
| 400_T5 | 2.083 | 2.082 |
| 400_T15 | 2.843 | 2.336 |
| 400_T30 | 2.325 | 1.583 |
| 400_T60 | 1.223 | 2.229 |

The ADI inflection point at 14:45 between the finer 400 m and 1200 m runs compared to the 3600 m runs is interesting to note. Looking at the best matched run at 14:45 (Fig.6), the fire is shown to be entering the start of its run along the heavily forested and steep escarpment. Fire spread prior to this point had been through a mix of grass, lightly forested areas and plantations across gently undulating land (Fig.7). From this point the fire spread uphill through rough and heavily forested terrain up to Mt Disappointment.

Figure 6. Yellow to red pixels showing modeled flame height with the white polygons of the reconstructed fire progression as of 14:45

**Figure 7.** Terrain profile of the approximate fire path from 14:45 to the top of Mt Disappointment, an increase in elevation of roughly 400m over 10 km.

With the increased slope and fuel load contributing to the fire spread, the Kilmore fire saw a significant increase in convective activity from this point generating a convective column well over 10,000 m in height. It is commonly accepted that large convective columns draw down winds from aloft to the ground. These upper winds are generally more consistent both in speed and direction when compared to lower level surface level winds (Fig.8, Fig.9).

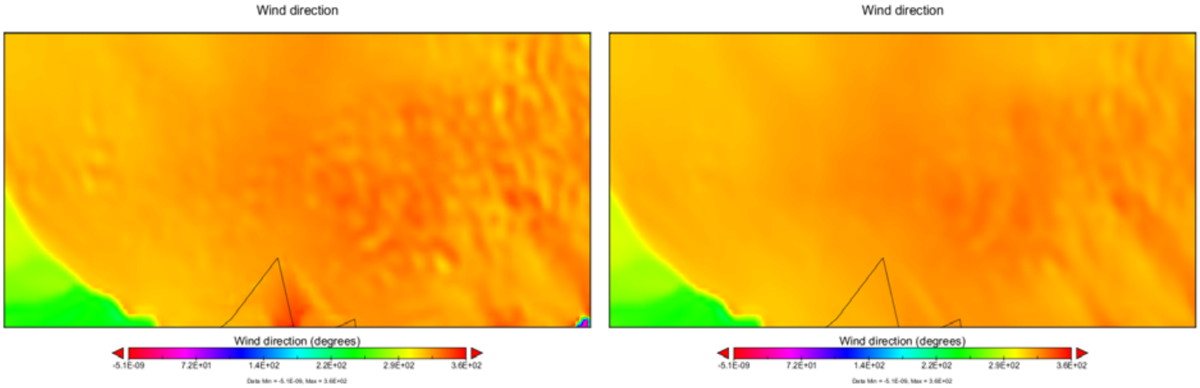

**Figure 8.** 3600 m ACCESS data showing wind direction over the general fire area at 14:00. Winds at 10 m above the ground (left) show significantly more directional variability compared to winds 250 m above the ground (right).

Figure 8 shows the difference in wind direction variability at 10 m and 250 m above the ground when modelled at 3600 m resolution. In the higher resolution 400 and 1200 m ACCESS data it is expected that this difference will be more pronounced, however only the 3600 m upper level wind data was available at this time.

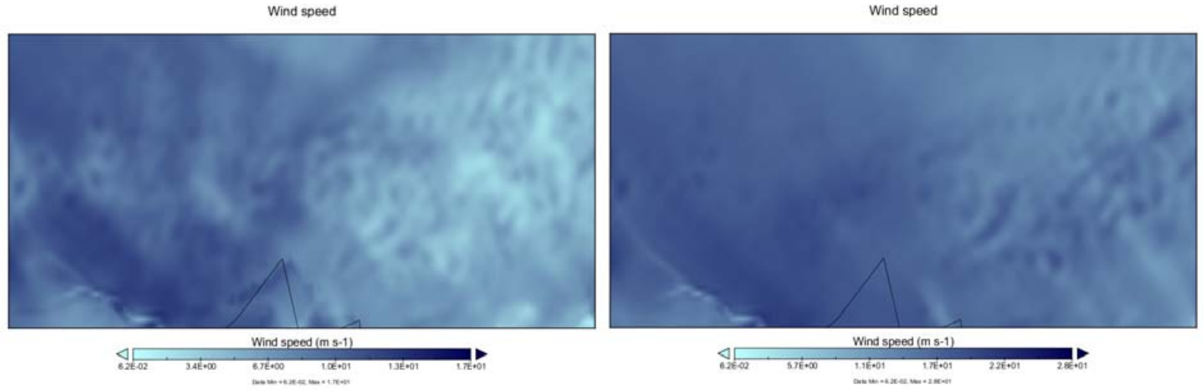

**Figure 9.** **3600 m ACCESS data showing wind speed over the general fire area at 14:00. Winds at 10 m above the ground (left) show significantly more variability compared to winds 250 m above the ground (right).**

General convention in bushfire fire spread modeling is to use 10 m winds in the calculation of spread rates. This is the standard height of the wind observations and forecasts. In the case of large fires with significant atmospheric coupling however, the use of observed or modeled 10 m winds is questionable given the drawing down of upper level winds by the convection column. For the purpose of fire spread modeling the winds applied would ideally be those at the active flaming zone.

Closer examination of modeled winds shows a pattern of increased variability with resolution which may explain the difference in PHOENIX results between higher resolutions and 3600 m data.

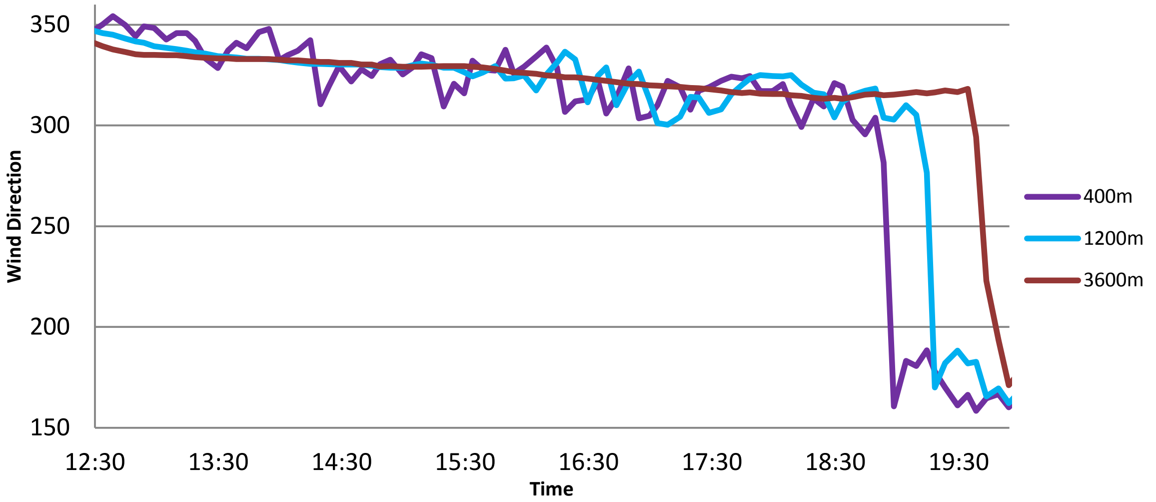

**Figure 10.** **Modeled (5 minute) wind direction data showing a general increase in variability with spatial resolution.**

Closer examination of the data reveals a further increase in wind direction variability commencing just after 14:45. This is particularly noticeable in the 1200 m resolution data where it transitions from a fairly linear pattern; this is repeated in the modeled wind speed data at approximately the same time.

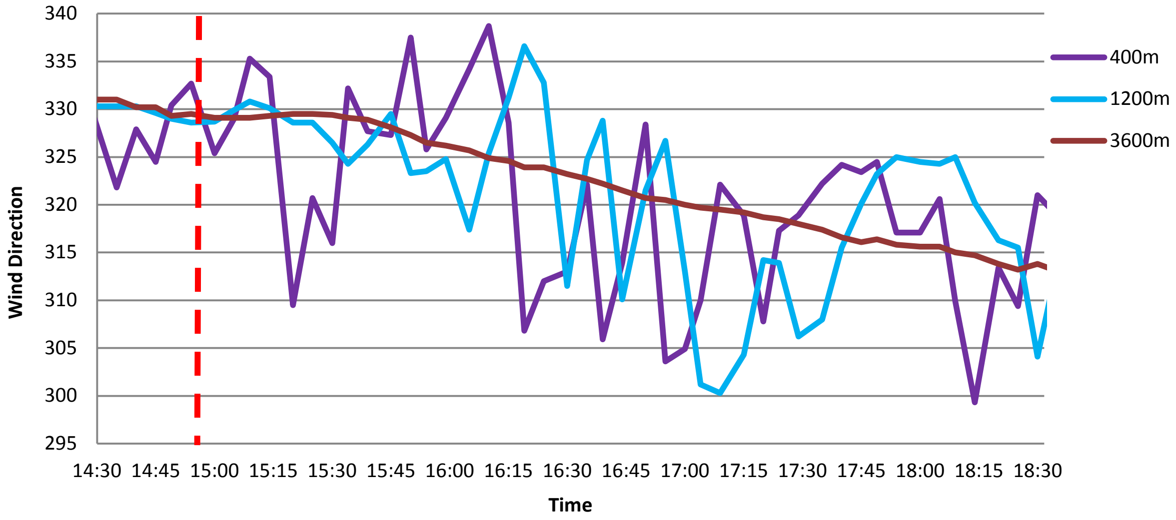

**Figure 11.** Closer view of modeled wind direction with the dashed red line indicating point (14:45) at which modeled wind direction variability begins to increase.

Wind direction variability can increase fire width, but at the cost of head fire spread rate, oscillating wind directions for a constant wind speed reduces the average wind speed in the average wind direction. This should coincide with a reduction in head fire spread rate assuming the fire is at or above its equilibrium head fire width.

A possible explanation for the sudden change in fire spread accuracy at 14:45 for the 400 m and 1200 m data is the increase in wind direction variability when compared to the 3600 m data. Assuming that the increased convective activity starting at approximately the same time began to draw down more directionally consistent air from aloft, a decrease in wind direction variation should apply. Looking closely at the uncoupled ACCESS modeled 400 m and 1200 m 10 m wind data shows an increase in directional variability rather than a decrease. Conversely, prior to this point the opposite should apply, which is the case with the higher resolution data, but not for the coarser 3600 m data.

Comparing the under and over estimate components of the ADI (Fig.12) shows the result of this. The directional variability prior to 14:45 gives the advantage to the 400 m and 1200 m data as it better reflects the gusty surface wind driven nature of the fire, however as the convective plume develops it begins to dominate localized weather around the head fire, drawing down more directionally consistent upper level winds and dampening directional variability on the ground which is better reflected by the smoother 3600 m data.

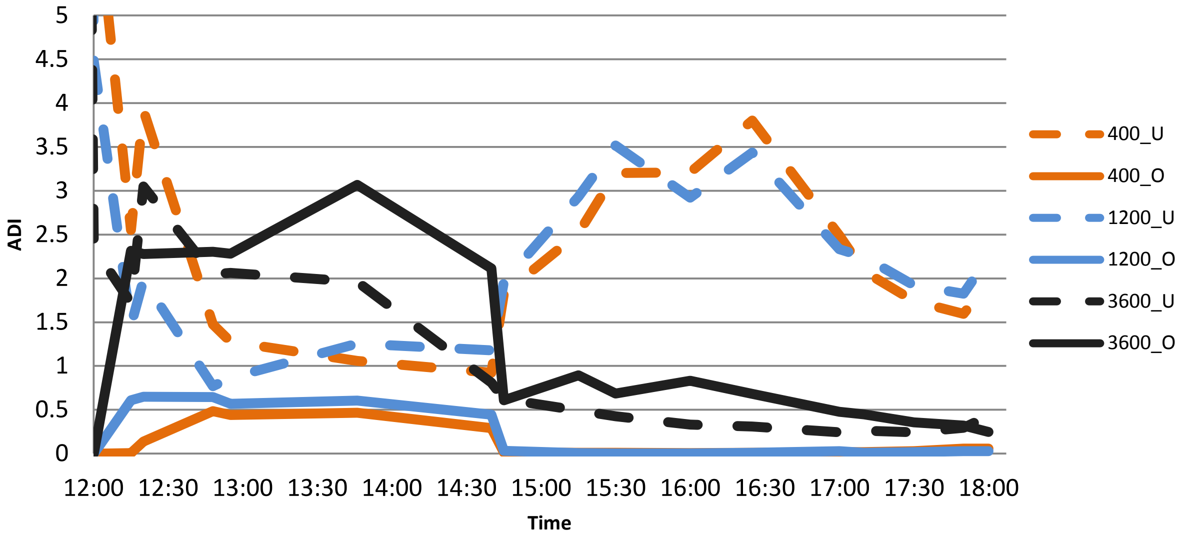

Figure 12. Over (solid lines) VS Under (dashed lines) estimated component ADI values showing 400 m and 1200 m data under predicting fire spread after 14:45. Conversely the 3600 m data over predicts spread rate up until 14:45

## Conclusions

The novel morphometric of Area Difference Index (ADI) was useful for comparing complex fire shapes predicted by PHOENIX and those reported by detailed fire reconstructions.

These conclusions relate to an analysis of a single fire event where the fire exceeded 100,000 ha in area and a convection column rising to about 10,000 m.

More detailed spatial and temporal weather prediction data did not necessarily result in better fire behaviour predictions as was expected. Early in the development of the 2009 Kilmore fire, 1200 m gridded weather data resulted in the best PHOENIX model output when compared with the reconstruction data. 400 m data was not as good and 3600 m data was worse again. However, once the fire became large (> 2,000 ha) and took in heavier fuels and steeper terrain, the 3,600 m weather data gave the best fire spread prediction in PHOENIX. This result is interpreted as small-scaled fires benefiting from finer spatial and temporal scaled weather forecast data, but for larger fires with a well established convection column, broader scaled weather forecast data better represents the conditions experienced by the fire.

Large bushfires interact with local weather, but this is not accounted for in routine weather forecast models. Coupled fire-weather models are capable of resolving the interaction of the two processes, but are computationally complex and slow.

The temporal resolution of the forecast weather data was less important than the spatial resolution in terms of its impact on fire spread predictions. Generally speaking, the 5 minute data could not be justified. The best fire spread predictions were generally with the 15 or 30 minute data.

Overall, the best final fire extent was predicted using the 30 minute, 3600 m data, but if the progression of the fire was of the greatest interest, then the 30 minute, 1200 m data was the best.

These results are likely to be different for smaller fires.

The higher spatial and temporal resolutions weather forecasts were very useful in identifying meteorological features not apparent at lower resolutions. The needs of a weather forecaster may not be the same as a fire behaviour modeller.

## References

Cui W, Perera AH (2010) Quantifying spatio-temporal errors in forest fire spread modelling explicitly. Journal of Environmental Informatics 16, 19-26.